Fragmentation studies with the CHIMERA detector at LNS in Catania: recent progress

A. Pagano[a], M. Alderighi[b],F. Amorini[c], A. Anzalone[c], N. Arena[a], L. Auditore[d], V. Baran[c], M. Bartolucci[e], I. Berceanu[f], J. Blicharska[g], J. Brzychczyk[h], A. Bonasera[c], B. Borderie[i], R. Bougault[j], M. Bruno[k], G. Cardella[a], S. Cavallaro[c], M.B. Chatterjee[l], A. Chbihi[m], J. Cibor[n], M. Colonna[c], M. D'Agostino[k], R. Dayras[o], E. De Filippo[a], M. Di Toro[c], W. Gawlikowicz[h], E. Geraci[k], F. Giustolisi[c], A. Grzeszczuk[g], P. Guazzoni[e], D. Guinet[p], M. Iacono-Manno[c], S. Kowalski[g], E. La Guidara[c], G. Lanzano['a], G. Lanzalone[c], N. Le Neindre[i], S. Li[q], S. Lo Nigro[e], C. Maiolino[c], Z. Majka[h], G. Manfredi[e], T. Paduszynski[g], M. Papa[a], M. Petrovici[f], E. Piasecki[r], S. Pirrone[a], R. Planeta[h], G. Politi[a], A. Pop[f], F. Porto[c], M. F. Rivet[i], E. Rosato[s], F. Rizzo[c], S. Russo[e], P. Russotto[c], M. Sassi[e], G. Sechi[b], V.Simion[f], K. Siwek-Wilczynska[r], I. Skwira[r], M. L. Sperduto[c], J.C. Steckmeyer[j], L. Swiderski[r], A. Trifirò[d], M. Trimarchi[d], G. Vannini[k], M. Vigilante[s], J. P. Wieleczko[m], J. Wilczynski[t], H. Wu[q], Z. Xiao[q], L. Zetta[e], W. Zipper[g]

[a]INFN, Sezione di Catania and Dipartimento di Fisica e Astronomia, Università di Catania, Italy

[b]INFN, Sezione di Milano and Instituto di Fisica Cosmica, CNR, Milano,Italy

[c]INFN, Laboratori Nazionali del Sud and Dipartimento di Fisica e Astronomia, Università di Catania, Italy

[d]INFN, Gruppo Collegato di Messina and Dipartimento di Fisica, Università di Messina, Italy

[e]INFN, Sezione di Milano and Dipartimento di Fisica Università di Milano, Italy

[f]Institute for Physics and Nuclear Engineering, Bucharest, Romania

[g]Istitute of Physics, University of Silesia, Katowice, Poland

[h]M. Smoluchowski Institute of Physics, Jagellonian University, Cracow, Poland

[i]Institute de Physique Nucléaire, IN2P3-CNRS and Université Paris-Sud, Orsay, France

[j]LPC, ENSI Caen and Université de Caen, France

[k]INFN, Sezione di Bologna and Dipartimento di Fisica, Università di Bologna, Italy

[l]Saha Institute of Nuclear Physics, Kolkata, India

[m]GANIL, CEA, IN2P3-CNRS, Caen, France,

[n]H. Niewodniczanski Institute of Nuclear Physics, Cracow, Poland

[o]DAPNIA/SPhN,CEA-Saclay, France

[p]IPN, IN2P3-CNRS and Université Claude Bernard, Lyon, France

[q]Institute of Modern Physics, Lanzhou, China

[r]Institute of Experimental Physics, Warsaw University, Warsaw, Poland

[s]INFN, Sezione Napoli and Dipartimento di Fisica, Università di Napoli

[t]Institute for Nuclear Studies, Swierk/Warsaw, Poland

The new detector CHIMERA, in its final 4π configuration, has been installed at Laboratori Nazionali del Sud (LNS) in Catania in January 2003. Beams of different energies ranging from protons to Au ions were delivered by the Tandem and the Super Conducting Cyclotron for nuclear reaction studies, in agreement with the approval of the Scientific Advisory Committee of LNS. Recent experimental results confirm very low energy thresholds of the trigger (below 0.5 MeV/nucleon), ensured within a wide dynamical range. Good characteristics of identification of light charged particles and heavy fragments have been obtained by using three detection techniques: ΔE-E, ΔE-time of flight, and the Pulse-Shape discrimination method. We present results of recent analysis concerning the production of intermediate mass fragments (IMF) in semi-peripheral collisions. Our results combined with theoretical Boltzmann-Nordheim-Vlasov simulations clearly demonstrate the presence of very fast processes of IMF production in the overlapping region of the target and projectile nuclei during re-separation, i.e. in the time scale comparable with the collision time. Evidence for slower, sequential-like production of IMF's is also shown.

1. Introduction

Production of fragments of intermediate mass (IMF) has attracted attention of nuclear physicists since a long time [1–3]. In recent years, multifragmentation processes in hot nuclei have been related to basic properties of the equation of state (EOS) of nuclear matter [4] and to a possible liquid-gas phase transition [5,6]. More recently, various topics such as influence of the isospin degree of freedom on the reaction mechanism [7], production of exotic nuclei [8], evolution of supernovae and the structure of neutron stars [9] significantly enlarged scientific interest in the studies of EOS. Our work concentrates on nucleus-nucleus collisions in the Fermi energy domain (20 MeV/nucleon $\leq$ E/A $\leq$ 100 MeV/nucleon). In this energy range, one can expect [10,11] a transition from one-body mean-field regime to two-body nucleon-nucleon interaction regime. A distinct feature in this transition range of energies is an abundant production of IMF's observed in the most violent nucleus-nucleus collisions. Much effort was devoted to understand the physics of this nuclear instability [12,13]. Disentangling of the initial dynamical stage of the collision from later stages characterised by the statistical decay of well defined equilibrated sources still remains a challenge in this field.

Recent activity of our group essentially was dedicated to advance our experimental methods and improve data analysis for studying this class of reactions. We will briefly review the progress in experimental techniques applied in CHIMERA, and in the following, some selected results concerning the IMF production in semi-peripheral collisions will be discussed. We note here that our recent activity also includes studies of central collisions [14] as well as a new project of upgrading the apparatus [15].

2. Experimental method

CHIMERA (Charged Heavy Ion Mass and Energy Resolving Array) was designed [16] for heavy-ion studies in the Fermi energy regime. In 1999, the forward part of the apparatus, made of 688 detection cells (CHIM688), arranged in nine rings covering the angular range from 1° to 30°, with full 2π azimuthal symmetry around the beam axis, was installed inside the reaction chamber CICLOPE at LNS in Catania. The rings were placed at variable distances from the target, ranging from 3.5 m (1°) to 1 m (30°). Isotopically enriched Sn projectiles were delivered to study the ^{124}Sn+^{27}Al and ^{112,124}Sn + ^{58,64}Ni reactions at the beam energy, E(^{112,124}Sn) = 35 MeV/nucleon. High granularity of the device was sufficient for nuclear studies in reverse kinematics. First report on the REVERSE experiment was given in Ref. [17]. In January 2003, the apparatus was completed by adding 504 detection cells, arranged in a spherical structure of a radius of 40 cm around the target. The sphere covers the detection angles between 30° and 176°. The single detection cell consists of a planar 300 μm-silicon detector (200 μm for the most forward ring) followed by a CsI(Tl) scintillator of the thickness ranging from 3 cm at backward angles to 12 cm at the most forward angles. Due to very compact mounting of the telescopes, the total geometrical efficiency of the system is about 95%. A recent view of the CHIMERA detector is shown in Fig. 1.

The front-end electronics architecture is constructed of compact (16 channels) NIM and CAMAC modules. The acquisition system is based on the FDL (Fast Data Link) connecting VME 9U DAQ system [18].

Beams of optimum intensities of $\sim 5 \cdot 10^7$ particles/s with typical burst frequency structure of $\sim$ 33MHz were used during the campaign. On the average, the overall time resolution, regarding the entire system of 1192 moduls, and accounting for both the beam burst jittering and detector time resolution, was as good as $\Delta T \approx 1$ ns, during most of the operation time of the LNS Super-Conducting Cyclotron. This result was achieved with the water-cooling system installed for temperature stabilization of the electronics (preamplifiers) under vacuum.

Three different detection techniques are simultaneously used in CHIMERA. First, the ΔE-E technique is employed for charge identification of heavy ions and for isotopic identification of IMF's with atomic number $Z < 10$. Second, mass identification is performed with signals from silicon detectors generating the time-of-flight signal (TOF), obtained by comparing the timing of the detector signal and the timing of the high frequency signal (HF) from the cyclotron. Third, energetic light charged particles (LCP), which are stopped in the scintillator crystal, are identified by applying the Pulse-Shape discrimination method using well shaped amplified signals generated by a 20 mm × 20 mm photodiode, optically coupled to the crystal. The identification characteristics achieved
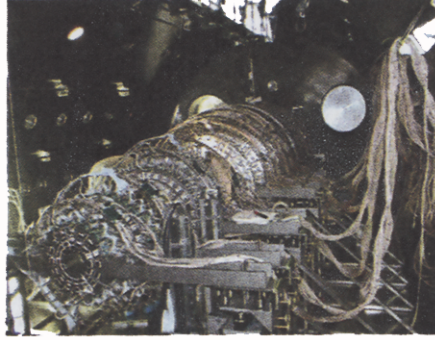
Figure 1. Recent view of the CHIMERA multidetector installed inside the reaction chamber CICLOPE at Laboratori Nazionali del Sud in Catania.

in the recent February-June 2003 campaign were very similar to ones already described in Refs. [17,19,20].

In the following section, we discuss results of recent analysis of semi-peripheral collisions in the ^{112}Sn + ^{58}Ni reaction (neutron poor) and ^{124}Sn + ^{64}Ni reaction (neutron rich) at 35 MeV/nucleon. For this study, we use only information obtained with the forward part of CHIMERA (CHIM688) during the first phase (April 2000) of the REVERSE experiment [17]. Events have been selected by requiring reconstruction of both total charge ($Z_{tot} \geq 40$) and total linear momentum ($|\vec{p}_{total}| \geq 60\%|\vec{p}_{beam}|$). Examples of distributions of these basic global variables for the ^{124}Sn + ^{64}Ni reaction at 35 MeV/nucleon are shown in Fig. 2.

3. Experimental results and discussion

In this section we concentrate on the analysis of semi-peripheral collisions, roughly selected by arbitrarily requiring that the multiplicity of charged particles, detected in a given event was less than five, $M_c < 5$. Under this condition, an intense group of events with the total charge close to the projectile charge ($Z = 50$) is clearly seen (see Fig. 2a). Moreover, for about 25% of these events with the reconstructed primary projectile-like fragment (PLF), also some remnants of the target nucleus (TLF) were detected in coincidence with the PLF.

In Fig. 3, some basic characteristics of the detected fragments are summarized for the neutron rich system ^{124}Sn + ^{64}Ni. (Similar results have been obtained for the neutron poor system ^{112}Sn + ^{58}Ni). In the upper left panel, the charge of the fragments is plotted as a function of their parallel velocity. In such a two-dimensional plot we can distinguish essentially three groups of fragments: PLF's (with $v_{par} > 6$ cm/ns), TLF's (with $v_{par} < 2$ cm/ns), and IMF's having intermediate velocities between the TLF and PLF components. In the upper right panel, the galilean invariant cross section in coordinates
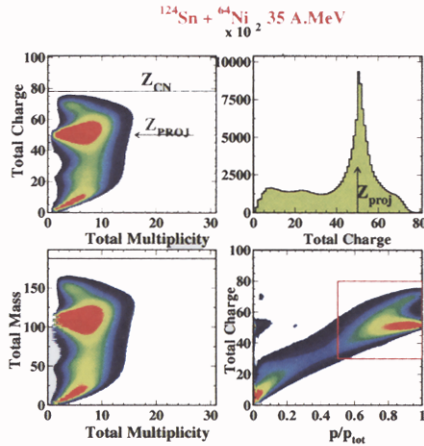
Figure 2. Distributions of some global variables: (a) and (c) the total charge and total mass as a function of the multiplicity of charged particles. Panel (b) shows the charge spectrum, and panel (d) the total charge vs. linear momentum correlation matrix.

V_{per} vs. V_{par} is shown for light fragments ($2 < Z < 13$), whereas, in the lower left panel the V_{par} distribution of these light fragments is plotted. The projectile velocity, V_p, mid velocity $V_{p/2}$, and the center of mass velocity, V_{cm}, are indicated in this panel. Finally, in the lower right panel we plot the charge distribution of the IMF's. This figure clearly shows that the charge distribution of the IMF's falls down with Z of an IMF nearly exponentially: Yield(IMF)$\sim \exp(aZ)$, with a value of the slope parameter $a = -0.22$. We found that a is rather independent of the IMF multiplicity. (This was checked for multiplicities $M_{IMF} \leq 3$.)

Our experimental results have been compared with theoretical predictions [21,22] based on the Boltzmann-Nordheim-Vlasov (BNV) transport theory. Results of the BNV calculations have been filtered to account for geometrical configuration of the detecting system. These results are superimposed on experimental distributions in Fig. 3 (green contours in upper panels, red histogram of the paralel velocity distribution of IMF's, and red symbols showing the predicted Z distribution of IMF's). Basic features of the PLF, TLF and IMF groups, which are best seen in the V_{par} vs. Z correlation plot, are perfectly reproduced by the BNV model. Amazingly, even the IMF charge distribution is quite accurately predicted.

Regarding the discrepancies between the theory and our data, it is obvious that the BNV model accounts only for relatively fast component of the IMF's due to the limited space and time of calculating the dynamical evolution of the system in each event. Therefore the model reproduces very well only the "prompt" component of IMF's, located approximately at the mid velocity, $V_{par} \approx 4$ cm/ns. These mid-velocity fragments are formed in the
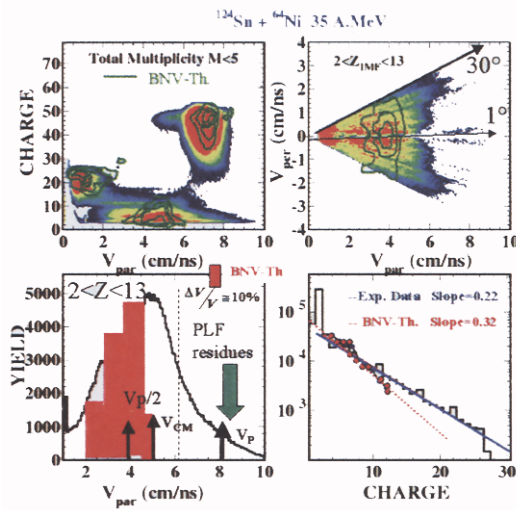
Figure 3. Results of the analysis of semi-peripheral collisions in the ^{124}Sn + ^{64}Ni reaction at 35 MeV/nucleon (see text).

neck region, practically within very short time of breaking up the system into two main fragments, PLF and TLF [21,22]. Sequential emission of IMF's at times longer than 300 fm/c after the collision could not be accounted for in the calculation. These "late" IMF's, originating from more or less sequential processes, considerably widen the range of the observed paralel velocities (see Fig. 3). In order to shed more light on the mechanism of the IMF production and the time scale of these processes, we selected in the upper left panel of Fig. 3 three two-dimensional regions enclosing rather unambiguously TLF's ($Z \geq 15$, 0.4 cm/ns $< V_{par} < 1.5$ cm/ns), PLF's ($Z \geq 30$, 6.0 cm/ns $< V_{par} < 8$ cm/ns), and IMF's ($3 \leq Z \leq 14$, 2.0 cm/ns $< V_{par} < 6.0$ cm/ns). For so defined fragments we calculated, event by event, the relative velocities in the IMF+PLF and IMF+TLF sub-systems, V_{rel}(IMF-PLF) and V_{rel}(IMF-TLF), respectively. Correlations [23] between these two quantities, normalyzed to the relative velocity corresponding to the Coulomb repulsion energy in a given sub-system, calculated with the Viola systematics formula [24] for asymmetric systems [25] are shown in Fig. 4. The IMF-PLF vs. IMF-TLF correlation of the reduced velocities is shown separately for three groups of IMF's: a) fast IMF's (4.5 cm/ns $< V_{par} < 6.0$ cm/ns), slow IMF's (2.0 cm/ns $< V_{par} < 2.5$ cm/ns), and medium velocity IMF's (2.5 cm/ns $< V_{par} < 4.5$ cm/ns). Position of group a) clearly suggests rather late, sequential decay of the primary PLF, because the relative velocity in the IMF+PLF sub-system is nearly equal to the velocity corresponding to the Coulomb

repulsion energy ($r_x \approx 1$). Similarly, group b) represents sequential decay of primary remnants of the target nucleus ($r_y = 1$). Finally, group c) corresponds to an intermediate situation when relative velocities in both sub-systems are small, that means that formation and separation of the IMF must occur when both PLF and TLF still remain at close distance. It is interesting to compare the correlation for group c) with results of the BNV simulation, shown in the inset d). Perfect agreement of these two correlation plots strongly supports the scenario of fast, dynamical production of IMF's in the overlapping region (neck) between target and projectile nuclei, in a time scale comparable with the collision time [21,22]. Our analysis shows that in addition to the prompt production of IMF's in the neck region, we also observe slower components originating from sequential decay of PLF's and/or TLF's when these primary fragments are already far away from each other.
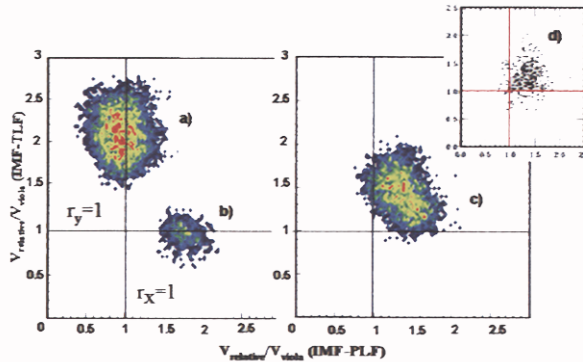

Figure 4. Correlation of the reduced relative velocities for the PLF+IMF and TLF+IMF sub-systems (see text). Plot 4d shows results of the BNV calculations [22]

Extension of our analysis for more dissipative collisions is in progress. Some preliminary results indicate that the dynamical IMF production mechanism [26–28,21,22] is present also in more central collisions, for larger particle multiplicities ($M_c \gg 5$), and for both neutron poor- and neutron rich systems investigated in the REVERSE experiment.

In conclusion, the excellent experimental characteristics of the new CHIMERA detector, in particular its capability to detect TLF's with good efficiency, give a unique opportunity to study the IMF production mechanism in heavy-ion collisions at the Fermi energy range. We have demonstrated in this work the coexistence of both dynamical and sequential mechanisms of the IMF production in nucleus-nucleus collisions at intermediate energies.

4. Acknowledgements

REFERENCES

1. R. Serber, Phys. Rev. 72 (1947) 1114.
2. G. Friedlander et al., Phys. Rev. 94 (1954) 727.
3. A.S. Goldhaber, Phys. Lett. 53B (1974) 306.
4. G. Sauer et al., Nucl. Phys. A 264 (1976) 221.
5. P.J. Siemens, Nature 305 (1983) 410.
6. J. Pochodzalla et al., Phys. Rev. Lett. 75 (1995) 1040.
7. Bao-An Li et al., Int. J. Mod. Phys. E7 (1998) 147.
8. P. Chomaz, C. R. Physique 4 (2003) 419.
9. C.J. Pethick and D.G. Ravenhall, NATO ASI Series C, 450 (1995) 59.
10. A. Bonasera, M. Di Toro and Ch. Gregoire, Nucl. Phys. A 463 (1987) 653.
11. G. Peilert, H. Stöcker and W. Greiner, Rep. Prog. Phys. 57 (1994) 533.
12. J. Richter and P. Wagner, Phys. Rep. 350 (2001) 1.
13. A. Bonasera et al., Rivista del Nuovo Cimento, 23 (2002) 1.
14. E. Geraci et al., Proc. of this conf.; E. Geraci et al., Nucl. Phys. A, to be published.
15. M. Alderighi et al., this conf. (poster presentation) and A. Alderighi et al., Nucl. Instr. Meth. A, to be published.
16. A. Pagano et al., Proc. 2nd INFN-RIKEN Symposium, Riken, May 1995 (eds. M. Ishihara, T. Fukuda, C. Signorini), World Scientific, p. 119; and S. Aiello et al., Nucl. Phys. A 583 (1995) 461.
17. A. Pagano et al., Nucl. Phys. A 681 (2001) 331.
18. E. De Filippo et al., Proc. 11-th IEEE INPS Real Time Conf., Santa Fe, June 1999, p. 78; and S. Aiello et al., IEEE Trans. on Nucl. Sci. 47 no. 2 (2000) 1.
19. N. Le Neindre et al., Nucl. Instr. Meth. A 490 (2002) 251.
20. M. Alderighi et al., Nucl. Instr. Meth. A 489 (2002) 257.
21. V. Baran et al., Nucl. Phys. A 703 (2002) 603.
22. V. Baran et al., arXiv:nucl-th/0309052 v1 19 Sep 2003.
23. J. Wilczynski, private coomunication, REVERSE coll., LNS Catania, May 2003.
24. V. Viola et al., Phys. Rev. C 31 (1985) 1550.
25. D. Hinde et al., Nucl. Phys. A 472 (1987) 318.
26. M. Colonna et al., Prog. Part. Nucl. 30 (1992) 17.
27. C.P. Montoya et al., Phys. Rev. Lett. 73 (1994) 3070.
28. J. Lukasik et al., arXiv:nucl-ex/0301018 v1 28 Jan 2003, and references therein.